The Dependence Of $Si/A_{III}B_V$ Light Source Photoluminescence Efficiency On Dynamic Displacements Of Atoms In The Crystal Lattice

Vladimir Osinsky, Petro Deminskyi, Natalia Lyahova,
Nina Syhoviy, Hooshmand Honarmand
Department of Optoelectronics, Institute of Microdevices NASU
Kiev, Ukraine
osinsky@imd.org.ua

Abstract – **The efficiency of light emitting diode (LED) depends on: (1) the choice of technological regimes; (2) temperature properties of the materials used to form heterostructures; (3) the concentration of defects in the grown films. Based on studies of standard dynamic displacements of atoms in the crystal lattice of GaN and $In_xGa_{1-x}N$ compared with AlGaInP solid solutions, we aimed to prove application of $In_xGa_{1-x}N$ for monolithic integration of $Si/A_{III}B_V$ RGB light sources in one technological process. We developed a software that allows you to specify the percentage distribution of the active layers for R, G, B - light radiation channels on the chip surface.**

Keywords—LED, light, dynamic displacements, $In_xGa_{1-x}N$, GaN, $Si/A_{III}B_V$, RGB, epitaxy, $A_{III}B_V$.

I. INTRODUCTION

Monolithic integration of RGB (red, green, blue) solid-state lighting is required in commercial, medical applications and has benefits compared with hybrid integration: simplified operating scheme, low driving currents, high switching speed, small size and low cost [1, 2]. Researches in the field of monolithic integration of light-emitting heterostructures led to the RGB-LEDs development using buffer and template nanolayers with specific properties via the control of III-nitrides and III-oxides growth.

To implement RGB light sources on a single chip and to get high flux of lighting and full color gamma of light emitting diode (LED) we need to develop: (1) the exact distribution of red, green, blue (RGB) LEDs on a chip surface, (2) the high-quality (defect-free) epitaxial structures with good crystal lattice matching of dissimilar materials [3].

Minimization of defects plays a decisive role in obtaining the reliability and high performance lighting system [3]. That is why we consider: (1) fundamental analysis for monolithic integration of light-emitting heterostructures which led us to study the influence of standard dynamic displacements of atoms in the III-N crystal lattice on the radiative recombination intensity, (2) the research in monolithic integration and as a result development of bases for creating RGB LEDs using $In_xGa_{1-x}N$.

Modern methods of micro- and nanostructures planar technology makes it possible to create a large number of planar p-n junctions with different topologies in a single chip that optimizes the flow of electric current and the output radiation of the LED structure. The generation of a wide spectrum of the mixed light from the chip requires creation of several grounds with different composition of solid-state compounds and energy bandgaps.

II. SOLID STATE SOLUTIONS FOR R, G, B ACTIVE LAYERS FORMING.

The researches in the field of solid solutions, including material properties of Ga-Al-In-N system for RGB LED applications, study opportunities in InGaN/GaN heterostructures creation due to unique physical properties of GaN and InGaN/GaN heteropair. InGaN bandgap can vary from 0.7 to 3.4 eV, expanding opportunities for their use [4].

We identified the expansion of long-wavelength part of the spectrum (5 nm/100K) and wavelength peak shift (3-10 nm/100K) that caused by recombination through dopant state inside the band-gap within the study of electroluminescence spectra of GaN films (Fig. 1) along the temperature -40 – +60 °C. During the research we use monochromator “MDG-23” and climatic heat-cold chamber “Mini Subzero MC71” [5].

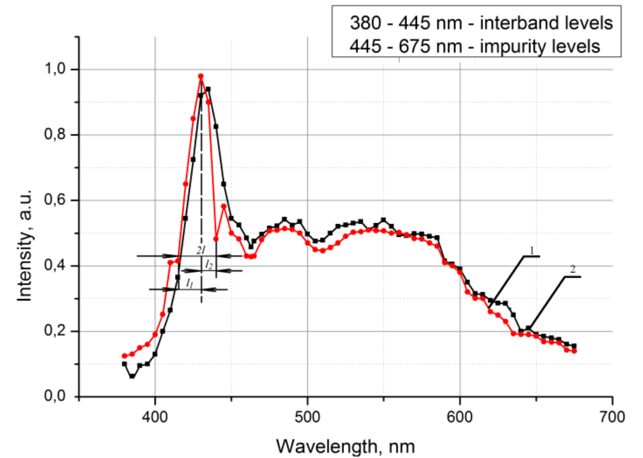

Fig. 1. Electroluminescence spectra of light emitting diode based on nitride gallium films. l_1 – harmonical part of spectrum, l_2 – unharmonical part of spectrum.1– *273 K, 2 – 333K.*

The spectral increasing intensity of the impurity levels is a result of increasing the temperature of the active region. The intensity of the spectrum is responsible for the interband transitions is reduced on 0.05 a.u./100 K due to the displacement of lattice atoms.

For determining the influence of the lattice dynamics at various temperatures we used calculation (1):

$$\sqrt{U^2_{dyn.}} = \frac{3h^2T}{4\pi^2 km\Theta^2}\left[D_n\left(\frac{\Theta}{T}\right)+\frac{\Theta}{4T}\right], \qquad (1)$$

of the standard dynamic displacements of atoms in the crystal lattice of GaN compound and InGaN solid solution for the first time. D_n - Debye function (determined for each value $x=\frac{\Theta}{T}$), Θ Debye temperature, k - Boltzmann constant, h - Planck's constant, m – the average effective ions mass.

We observed major differences between AlInGaP and InGaN that give reason for replacement AlInGaP with $In_{30\text{-}40}Ga_{70\text{-}60}N$.

Several reasons led us to this conclusion: (1) the dynamics of the crystal lattice of GaN are twice as more stable as InP at similar temperatures (Fig. 2); (2) the radiation intensity of the InP films falling twice compared to GaN in the range of -40 °C +60 °C.

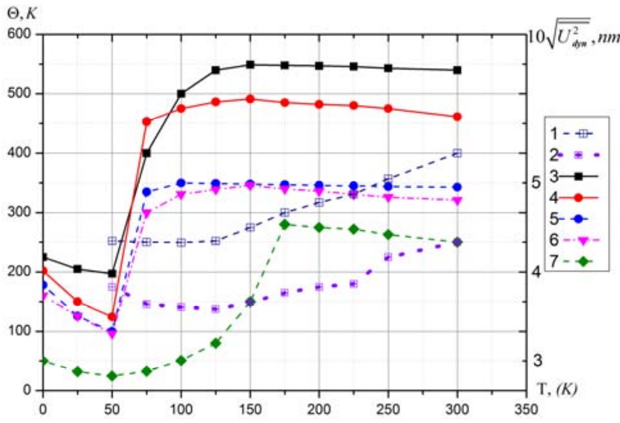

Fig. 2. Dependence of the Debye temperature (InP – 1; AlGaInP – 2; GaN – 3; InGaN – 4; GaAs – 5) in the AlGaInNRAs system and standard dynamic displacements of atoms ($U^2_{dyn.}$) for AlGaInP (6) and GaN (7).

The intensity of radiative recombination decreases exponentially with increasing temperature, which corresponds to increase of standard dynamic displacements of atoms of the crystal lattice. Between the fractional quantum efficiency of radiative recombination and standard dynamic displacement exists relationship (2):

$$\ln\frac{1}{\Phi} = A + R\sqrt{U^2_{dyn.}(T)}, \qquad (2)$$

where Φ - the intensity of recombination radiation, A - characteristic of the intensity in the absence of lattice vibrations T – temperature, R - coefficient depending on the concentration of impurities and defects specific recombination mechanism. Due to these we see less fractional quantum efficiency dependence of GaN compound to standard dynamic displacements compared to AlInGaP solid solution (Fig. 3).

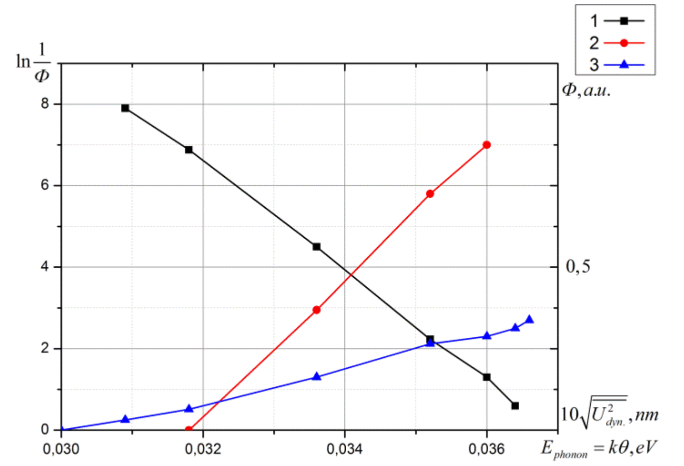

Fig. 3. Phonon energy dependence of the fractional quantum efficiency of radiative recombination of indium phosphide (1), the standard dynamic displacements of atoms of the crystal lattice of AlGaInP (2) and GaN (3).

Implementation of several InGaN light emitting channel with a different band gap in microcluster structures allows to produce structures capable of emitting in the visible wavelength range [6, 7] that promotes processing integration of RGB LED structures on a single chip. Advantages of using the same type of solid solutions of InGaN are: (1) reducing the amount of technological operations; (2) using the same reagents and similar technological process and conditions inside the epitaxial reactor during the manufacturing process.

Despite these, one of the main problems in the technology of RGB light source creation onto a single chip with InGaN as the active layer for three channels LEDs making is an increase in indium content in $In_xGa_{1-x}N$ [8, 9]. The shift to longer wavelengths of radiation caused significant mismatch of the lattice parameters in the system of GaN-InN (10.7% to a 15.0% for the *c* lattice parameters, respectively) [10].

A large difference in the lattice parameters leads to two important effects: (1) initiation of significant mechanical stress due to a different radiation range in the crystal lattice of the ternary compound InGaN provided phase disintegration of the solid solution. (2) even a low concentration of In in the InGaN layer, strongly alters the lattice constant of InGaN compared with GaN, resulting in a high degree of strength of InGaN.

III. PERCENTAGE DETERMINATION OF RGB CHANNELS ON ONE CHIP.

For determination the percentage ratio between the RGB channels of radiation we use five samples of GaN (blue), InGaN (green), AlInGaP (red) 1×1 mm LEDs. On the base of a red, green and blue LEDs, chromaticity coordinates for x, y and Mack Kami equation (3) (absolute maximum error of about 2 K) we calculated the Correlated Color Temperature for one RGB light emitting chip in the range 2856–6500 K (in accordance with the ICE D65 light sources) [11].

$$CCT = 449n3 + 3525n2 + 6823.3n + 5520.33, \qquad (3)$$

where n = (x − 0.3320) / (0.1858 − y).

On the base of transformation matrix equations for different light sources, the coefficient n takes the form (4):

$$n = ((0.23881)R + (0.25499)G + (-0.58291)B) / ((0.11109)R + (-0.85406)G + (0.52289)B). \qquad (4)$$

Through the: (1) algorithm for calculating the color temperature (2) the percentage of R, G, B channels, (3) experimental structures, and on the basis of the study of light-emitting characteristics, such as candle per square meter, candle-power and brightness it is possible to receive the required color temperature, as well as the color rendering index.

We calculated the color temperature in this approximation – 3224 ± 2K that corresponds to the percentage of 28% (R) : 71% (G) : 1% (B). For percentage of 15% (R): 81% (G): 4% (B) color temperature - 3614K ± 2K.

The color temperature that corresponds to the percentage values between light emission RGB-channels enables to define the uniform distribution of each R-, G-, B- channels on the chip surface of specified sizes. For this functionality we implemented a software (Fig. 4). The program manually sets: chip size; pores size (diameter), the distance between the pores, the distance between the R, G, B-light emitting channels; substrate diameter, thickness of the slash between the chips, the percentage of red, green and blue channels; side of the square (LED chip) on the graph (for clarity).

The software makes it possible to:

- Count the number of LED chips onto the substrates with the dimensions specified in the program, taking into account the thickness of the slash between grown LED chips.
- Estimate count (calculation error ~ 10 %) amount of nanopores with technological route.
- Specify the percentage distribution of the active layers of each of the ternary channels over the chip surface.
- Calculate the microcluster structure.
- Specify the masks thickness of necessary/possible length and width for mask opening for refill-deposition of certain area of one of three active layers under certain process conditions.

Dispensing accuracy depends on the quality of the buffer layer with the nanopores and is equal to ~ 7 %, which was found as a result of evaluating the quality of the obtained films.

IV. GaN NANOSTRUCTURES FOR HIGH EFFICIENCY LEDS

InGaN/GaN multiple quantum wells (MQWs) are usually used as the active layers in GaN LEDs because of their high radiative recombination efficiency and their capability of emitting in a spectral range which can cover almost the whole visible spectrum. For high power applications GaN-based LEDs will be run at very high current densities where threading dislocations may shorten the lifetime of the devices. Also, threading dislocations may be a vibrant stair towards improving the efficiency of nitride LEDs.

Blue LEDs based on InGaN already reached external quantum efficiency of over 70%, but it is significantly reduced in the yellow - green range. Particularly, because of the contribution of the intense piezoelectric fields (≈ 0.3 - 1.5 MV / cm), attributed to polar (0001) crystallographic orientation along which GaN/InGaN QW is still mainly grown. Indium incorporation is harder in polar than in non polar and semi polar plane.

We have demonstrated the growth of high quality GaN layers (3 μm-thick) developed by metal organic chemical vapor deposition (MOCVD) grown at 1020°C on the nonpolar α-GaN (11 2 0) layer grown by the hydride vapor phase technique on (100) Si substrate templated by porous anodized aluminum oxide (AAO) mask. Characterization of the initiation layer (Al_2O_3) was carried out by means of atomic force microscopy based on scanning probe microscope NanoScope IIIa. [12, 13]

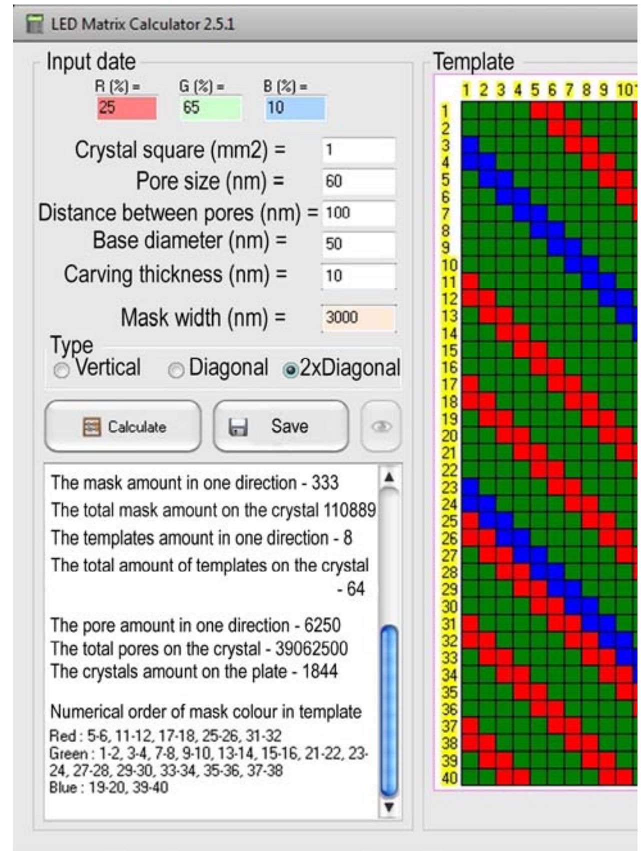

Fig. 4. Interface software to calculate the distribution active layer on the crystal surface.

Then, a layer of SiO_2 (0,1μm) was deposited on the top of GaN by plasma enhanced chemical vapor deposition (PECVD). To fabricate nanopore mask, the $Si0_2$ surface was patterned by using AAO as an etch mask. Pattern assignment from the AAO template to the SiO_2 film, was achieved through CF_4 - based inductively coupled plasma (ICP) etching. After pattern transfer to the $Si0_2$ layer, the AAO template was selectively etched away in 5% phosphoric acid. The average pore diameter was ~ 65 nm with an interpore distance of ~ ll5 nm. Organic contaminants were removed in acetone. The nano patterned samples were first annealed in N_2 ambient for 3 minutes at 1010°C in the MOCVD reactor to remove any surface destruction produced by ICP etching. Nano epitaxial lateral GaN overgrowth is developed by MOCVD through the nano pores of SiO_2. Trimethylgallium (TMGa), and NH_3 were used as the Ga and N sources, respectively. At growth pressure of 65 Torr and growth temperature of 1010°C, the carrier gas was N_2. The reactor temperature was released to 760°C and 4 periods of InGaN/GaN MQW were grown on the GaN nanorods, trimethylindium (TMIn) was used as the In source.

The thickness of the barrier and the well were ~ 30Å and 45Å, respectively, which were determined by transmission electron microscopy (TEM).

In the study of GaN nanorod arrays with TEM, it was found that the nanorods had vertical side walls of the SiO_2 pores mask. Their height was determined by the thickness of the mask. Deposition of gallium nitride above masks were not observed due to its low coefficient of adhesion to SiO_2, Fig.5, a.

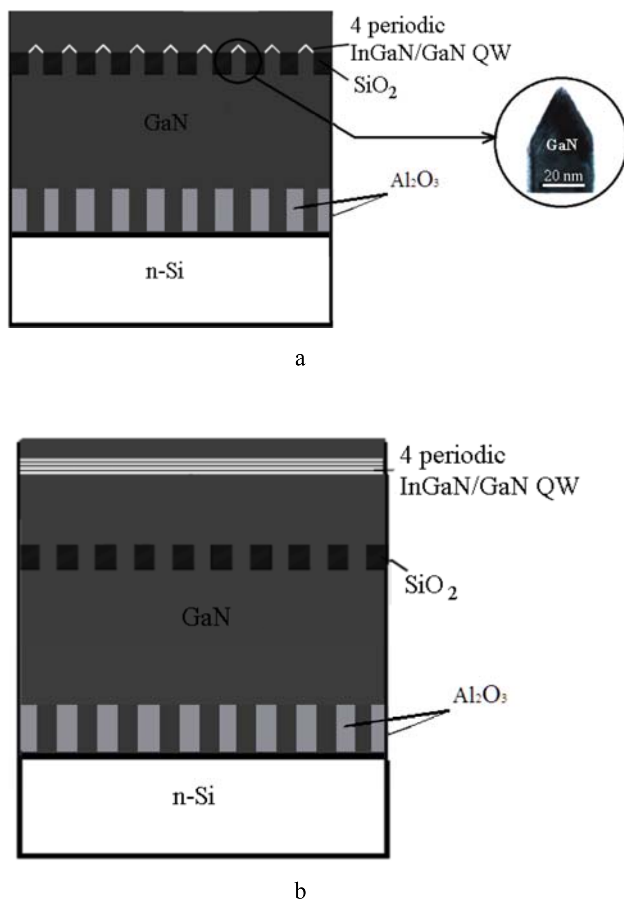

Fig 5. a - GaN/InGaN MQW (molecular quantum well) on the system of nanorods; b - GaN/InGaN MQW on "planar " GaN template layers (control structure).

Optical performances of InGaN/GaN MQWs structures shown in Fig.5, were investigated by the micro-PL spectrum (shown in Fig.6). Strong emission around 500nm was observed from the InGaN/GaN MQWs grown on the GaN nanorods. In contrast, the emission from the control “flat” InGaN/GaN MQWs was an order of magnitude lower in intensity. This intensity enhancement is attributed to reduce the number of nonradiative recombination centers associated with threading dislocations. Furthermore, InGaN/GaN MQWs were grown on facet. The faceted structures on top of nanorods reduce internal light reflection and distribute the light outer, improving the light extraction efficiency. Also the emission peak from the MQWs grown on the GaN nanorods was shifted by ~38nm compared with control MQWs sample on “flat” layer because of higher In arrangement in the MQWs. The strain in the GaN layer has an obvious effect on the In incorporation during the InGaN growth. Under the growth of InGaN layer on “flat” GaN, the compressive strain often hampers the integration of In atoms into the InGaN lattice.

InGaN/GaN MQWs on arrays of nanorods have the following advantages over MQWs on conventional "flat" films:

- Lower dislocation density, which leads to increased internal quantum efficiency;
- The possibility of greater indium incorporation in the solid solution;
- Light extraction increasing.

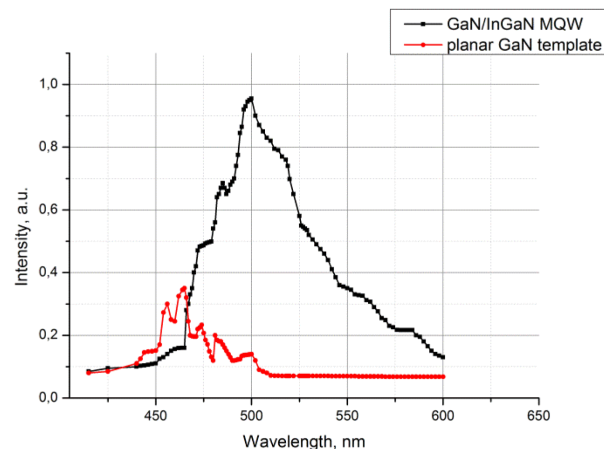

Fig. 6. Photoluminescence GaN / InGaN MQW nanorods on the system (solid line) and the "planar» GaN template layers (dashed line).

V. CONCLUSION

We found that the radiation intensity with temperature in the range of -40 °C +60 °C decreases in GaN two times less than in InP and proved the practicability of replacing the commonly used solid solutions AlInGaP on $In_xGa_{1-x}N$ with indium content ~ 30-40%. This provides RGB emitters integration in a single process.

We created the software application with a graphical interface that allows to simulate the distribution of RGB microcluster structures on the surface of structured one-chip buffer nanolayers, and counts the number of LED chips on substrates given diameter, the approximate area of nanoporous structures (~ 10%), taking into account technological route and rely the masks structure for RGB white light source on Si.

As for GaN nanostructutes for high efficiency LEDs, it has been demonstrated that InGaN/GaN MQWs on arrays of nanorods have the lower dislocation density, which leads to increased internal quantum efficiency; the possibility of greater indium incorporation in the solid solution; light extraction increasing.

REFERENCES

[1] I.V. Masol, V.I. Osinsky, O.T. Sergeev, Information Nanotechnology. Makros, Kyiv, 2011 (in Russian).

[2] V.I. Osinsky, D.I. Murchenko, H. Honarmand, “Si/A3B5 one chip integration of white LED sources”, Semiconductor Physics, Quantum Electronics & Optoelectronics. − 2009. V. 12, N 3. P. 240-250.

[3] Osinsky V., Osinsky A., Miller R. "1963 InGaAsP to Today's AllnGaNAsP Alloy for LED and Laser Applications" LED 50th Anniversary Symposium October 24 & 25, 2012 Urbana-Champaign, Illinois, USA

[4] Goriunova N.A. Diamond-like semiconductor compounds. Sovetskoie Radio, Moscow, 1968, p. 268 (in Russian).

[5] V. Osinsky, P. Deminskyi, “Si/A3B5 integrated light sources: the third stage of informatization”, VI International conference of optoelectronic information technology «PHOTONIC – ODS 2012», Vinnitsya, 2012, p. 45

[6] S. Nakamura, S. Pearton, and G. Fasol, “The Blue Laser Diode: The Complete Story” Springer-Verlag, Heidelberg, 2000.

[7] T. Kuykendall, P. Ulrich, S. Aloni, and P. Yang, Nature Mater. 6, 951 2007.

[8] E. Fred Schubert, “Light-Emitting-Diodes, Second Edition” (2006)

[9] Moses P. G., Van de Walle Chris G. Band bowing and band alignment in InGaN alloys / P. G. Moses, Chris G. Van de Walle // Appl. Phys. 96. - 2010. – P. 21908

[10] O Ambacher "Growth and applications of Group III-nitrides" J. Phys. D: Appl. Phys. 31 (1998) 2653–2710.

[11] C. S. McCamy “Correlated color temperature as an explicit function of chromaticity coordinates”, Color Research & Application. – 1992. – Vol. 17(2). – Pp. 142–144.

[12] V.Osinsky, V.A. Labunov, G.G. Gorokh, N. N. Lyahova, N.O. Lyahova, D.V. Solovey, “Template layers for Si/A3B5 nanostructures”, Electronics and signal, «Problems of electronics». – 2008. – №1 – 2. – C. 76–90.

[13] A. Polyakov, V. Osinsky, G. Gorokh, N. Lyahova, etc. “Nonpolar GaN grown on Si by hydride vapor phase epitaxy using anodized Al nanomask”, Appl. Phys. Lett. - 2009. – V. 94. – №2.

[14] V. Osinsky, N. Kostykevich “Integral optron”, AC №551730 (USSR), priority 1973 г.

[15] V. Osinsky, F. Kacapov, “GaAs epitaxy in windows of Si surface”. Thesises of Belarus Science Academy, 1978, V. 12., № 2, Pp.123-126.

[16] V. Osinsky, O. Privalov, O. Tuhonenko, “Optoelectronic structures on multicomponent semiconductors – Science and engineering, 1981. – P. 208

[17] V. Osinsky, “Integration of LED and transistor microstructures of solid state sources”, Thesis of V International scientific conference «Electronics and informatics 2005». – Moscow-Zelenograd. – 2005. – V.1. – Pp. 260–261.

[18] V. Osinsky, T. Katsapov, E. Tyavlovskaya. “Structural perfection of selective GaAs regions in Si-substrate windows” / – Phys. Stat. Sol. – 1984. – Vol. 82, №2. – P. 174–177.

[19] Osinsky V., P. Oleksenko, V. Verbitsky, “Problem with integration heteroelectronic structures with Si IC” Technology and design in electronic application. – 1999. – №1. – Pp. 3–17.